MUSCULOSKELETAL

CrossMark

Diffusion tensor imaging of articular cartilage using a navigated radial imaging spin-echo diffusion (RAISED) sequence

Alejandra Duarte[1] · Amparo Ruiz[1] · Uran Ferizi[1] · Jenny Bencardino[1] · Steven B. Abramson[2] · Jonathan Samuels[2] ·
Svetlana Krasnokutsky-Samuels[2] · José G. Raya[1]

Abstract

Objective To validate a radial imaging spin-echo diffusion tensor (RAISED) sequence for high-resolution diffusion tensor imaging (DTI) of articular cartilage at 3 T.

Methods The RAISED sequence implementation is described, including the used non-linear motion correction algorithm. The robustness to eddy currents was tested on phantoms, and accuracy of measurement was assessed with measurements of temperature-dependent diffusion of free water. Motion correction was validated by comparing RAISED with single-shot diffusion-weighted echo-planar imaging (EPI) measures. DTI was acquired in asymptomatic subjects ($n = 6$) and subjects with doubtful (Kellgren-Lawrence [KL] grade 1, $n = 9$) and mild (KL = 2, $n = 9$) symptomatic knee osteoarthritis (OA). MD and FA values without correction, and after all corrections, were calculated. A test-retest evaluation of the DTI acquisition on three asymptomatic and three OA subjects was also performed.

Results The root mean squared coefficient of variation of the global test-restest reproducibility was 3.54% for MD and 5.34% for FA. MD was significantly increased in both femoral condyles (7–9%) of KL 1 and in the medial (11–17%) and lateral (10–12%) compartments of KL 2 subjects. Averaged FA presented a trend of lower values with increasing KL grade, which was significant for the medial femoral condyle (-11%) of KL 1 and all three compartments in KL 2 subjects (-18 to -11%). Group differences in MD and FA were only significant after motion correction.

Conclusion The RAISED sequence with the proposed reconstruction framework provides reproducible assessment of DTI parameters in vivo at 3 T and potentially the early stages of the disease in large regions of interest.

Key Points
• *DTI of articular cartilage is feasible at 3T with a multi-shot RAISED sequence with non-linear motion correction.*
• *RAISED sequence allows estimation of the diffusion indices MD and FA with test-retest errors below 4% (MD) and 6% (FA).*
• *RAISED-based measurement of DTI of articular cartilage with non-linear motion correction holds potential to differentiate healthy from OA subjects.*

Keywords Articular cartilage · Diffusion tensor imaging · Osteoarthritis · Reproducibility of results · Magnetic resonance imaging

Abbreviations

CV	Coefficient of variation
DTI	Diffusion tensor imaging
EPI	Echo-planar imaging
FA	Fractional anisotropy
FT	Femoral trochlea
KL	Kellgren-Lawrence score
LFC	Lateral femoral condyle
LT	Lateral tibia
MD	Mean diffusivity
MFC	Medial femoral condyle
MRI	Magnetic resonance imaging
MT	Medial tibia
OA	Osteoarthritis
P	Patella
PG	Proteoglycan

✉ José G. Raya
Jose.Raya@nyumc.org

[1] Center for Biomedical Imaging, Department of Radiology, New York University Langone Health, 660 First avenue, 4th Floor, New York, NY 10016, USA

[2] Division of Rheumatology, Department of Medicine, New York University Langone Health, New York, NY, USA

RAISED	Radial imaging spin-echo diffusion tensor
SE	Spin echo
SNR	Signal-to-noise ratio

Introduction

Diffusion tensor imaging (DTI) of articular cartilage is a novel application that has the potential to assess compositional and structural properties of articular cartilage as a biomarker for osteoarthritis (OA) [1–7]. In vivo measurement of DTI of the articular cartilage is technically challenging due to the requirements of spatial resolution (~0.6 mm in-plane) and the short T2-relaxation time of cartilage (~30 ms). Thus, it has not been until recently that first studies have shown diagnostic value of DTI for OA, first at high fields (7 T) and later at 3 T [8–10]. Spin-echo (SE)-based sequences offer many advantages in performing DTI of articular cartilage since they provide excellent image quality, have SNR efficiency, and are insensitive to B0 and B1 inhomogeneity [11]. The principal drawbacks of SE sequences are their long acquisition times, and sensitivity to motion due to its sequential acquisition of the k-space.

To overcome these limitations, we implemented a radial imaging spin-echo diffusion tensor (RAISED) pulse sequence. The RAISED pulse sequence uses a radial acquisition that allows for higher undersampling rates (acceleration factor) as compared to Cartesian acquisition while preserving image quality. To avoid motion artifacts caused by the diffusion gradients, a 2D echo-planar readout was added after each radial acquisition (spoke) for non-linear motion correction [12]. Since articular cartilage is only a few millimeters in thickness, a careful validation of RAISED sequence is required to demonstrate that it can perform accurate measurements. Particularly problematic, is the presence of eddy currents that can cause both geometric distortion and changes in the signal intensity depending on the polarity of the diffusion gradients.

The purpose of this work was to investigate the feasibility of DTI of articular cartilage at 3 T using the RAISED sequence. In particular, our objectives were to (1) validate the RAISED sequence in phantoms for accuracy and robustness; (2) establish the technical feasibility of RAISED for in vivo imaging on healthy controls and OA subjects.

Materials and methods

MRI protocol

MRI was performed on a 3 T whole-body MRI scanner (Prisma Magnetom, Siemens Healthineers) using a birdcage transmit, 15-channel receive knee coil from the same vendor.

The RAISED sequence is shown in Fig. 1a. The sequence includes a non-selective fat-saturation block with a spin-echo diffusion-weighted preparation, followed by a radial readout and a monopolar 2D echo-planar imaging (EPI) acquisiton for non-linear phase correction. In particular, the RAISED images were acquired with a TE/TR = 39/1400 ms using 105 radial views (spokes) per slice with a bandwidth of 280 Hz/pixel. Fifteen sagittal slices were acquired from each subject with a slice thickness of 3 mm and an in-plane resolution of 0.6×0.6 mm^2 (208×208 acquisition matrix). One b_0 image and six diffusion-weighted images with a b value of 300 s/mm^2 were acquired ($\Delta = 14$ ms, $\delta = 9$ ms, six directions obtained from Downhill Simplex Minimization, DSM-6 [13]) with acquisition time 17:50 min. The navigator was acquired

a RAISED pulse sequence
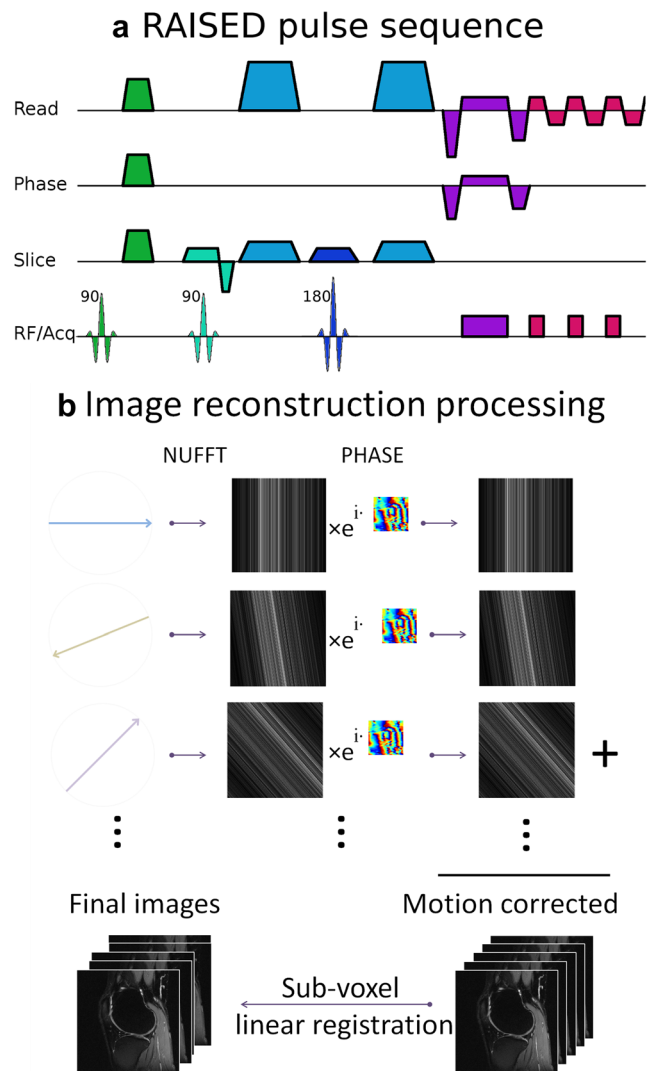

b Image reconstruction processing

Fig. 1 **a** Diagram of the RAISED sequence that includes a fat saturation block (light green), followed by a 90 degree excitation (cyan), diffusion encoding (light blue), refocusing (dark blue), diffusion de-coding (light blue), readout (purple), and EPI navigator (red). The readout gradients change orientation for all acquisitions. **b** Summary of the image reconstruction pipeline for the RAISED data including non-linear phase correction and image registration

with a 32×32 matrix (4.8×4.8 mm^2) using a monopolar EPI readout with a bandwidth of 800 Hz/Px and a partial Fourier of 6/8. The imaging protocols for phantom and in vivo clinical scans were the same, but the TR of phantom imaging was reduced to 1150 ms in order to provide a similar SNR to that of in vivo measurements. All knee images were acquired in the sagittal plane-oriented perpendicular to the tangent line to the posterior aspects of the femoral condyles.

Sequence validation

RAISED was validated for accuracy of water diffusion data at different temperatures, starting from room temperature (17 °C) to 38 °C. For room temperature measurements, the phantom was kept in the MRI scanner suite for at least 24 h before MRI. The water phantom was heated on an incubator for at least 2 h and placed in an insulating recipient for MRI. Phantom temperature was measured with a laser thermometer just before the MRI scan. Our diffusion measurements were compared to published measurements of water diffusivity in a similar range of temperatures, [14–17] using an Arrhenius plot available online [18].

We tested the sensitivity of the RAISED sequence to eddy currents. Depending on the polarity of the diffusion gradients, eddy currents can cause changes to the signal intensity, as well as geometric distortions [19, 20]. In particular, we looked for differences in signal intensity or geometric distortions between images acquired with opposite diffusion gradient-encoding polarities. Diffusion-weighted images were acquired with the gradients in two polarities along each direction in the magnet reference system ($\pm X$, $\pm Y$, $\pm Z$). For each diffusion polarity, three repetitions were acquired. All images were acquired transversal to the phantom. The average signal intensity was calculated in a region of interest placed in the center of the phantom (kept the same for all measurements). For each direction (X, Y, Z), we tested if the difference in average signal between images acquired with different polarities (e.g., $+X$ and $-X$) were the same as the differences between repetitions with the same direction and polarity (e.g., $+X$ and $+X$).

Geometrical distortions were assessed using our segmentation tool that allows for accurate sub-voxel segmentation [21]. The segmentation program generates a polygonal contour around the phantom with points placed at a distance less than 0.5 voxel size. The geometric difference of two segmentations was calculated as the average minimum distance of each point in the contour of one segmentation to all the contour points in the second segmentation. We tested if the geometric difference between segmentations of images acquired with different polarities was significantly larger than the geometric differences between segmentations of images acquired with the same polarity.

Finally, we tested that the motion-corrected diffusion values measured in vivo are not biased compared to a single-shot EPI sequence unaffected by motion. EPI and RAISED sequences were acquired in the right calf muscle of three healthy volunteers with the same diffusion parameters as in cartilage measurements (b value = 300 s/mm^2, $\Delta = 14$ ms, $\delta = 9$ ms, 6 directions DSM-6) and identical resolution (1.6×1.6 mm^2). We use the calf since EPI in joints have sub-optimal resolution for the thin cartilage (~ 2 mm) and is affected by off-resonance artifacts. ROIs were drawn in the soleus and the gastrocnemius muscle groups on the RAISED b_0 images. The same ROIs were used for the EPI images after visual inspection that any artifact affected ROIs in EPI images. For each ROI, the mean MD and FA was calculated using the parameter maps obtained from EPI, RAISED without motion correction, and RAISED after motion correction.

Participants

MRI of the dominant knee was performed on six volunteers and on the symptomatic knees of 18 patients with tibiofemoral knee OA. Volunteer exclusion criteria were any episodes of continued knee pain in the past 3 years and any history of knee surgery or trauma. OA patients in the cohort had to fulfill the clinical criteria of the American College of Rheumatology or the diagnosis of knee OA [22]. Exclusion criteria were any contraindication to MRI, pregnancy, history of any other form of arthritis, and administration of hyaluronan or corticosteroid injection to the affected knee in the 3 months before MRI. Standardized X-rays using the Syna-Flexer® position frame were available from the subjects within 1 week of the MRI. Kellgren-Lawrence (KL) grade was assessed in X-rays [3]. A subset of three healthy and three OA subjects were scanned three times to assess test-retest reproducibility. The first two scans were acquired back-to-back allowing for patient reposition between scans. The third scan was acquired a week later. The study was approved by the Institutional Review Board and performed in compliance with HIPAA regulations. All subjects provided written informed consent.

Image processing

For motion correction RAISED reconstruction, we used the method described in Miller et al (Fig. 1b) [12]. Briefly, the 2D back projection was calculated for each spoke, from which the phase of the 2D EPI navigator was subtracted. For each received channel, an image was generated by summing all motion-corrected back projections and the final image was calculated as the sum of squares over all channels.

The last step of image reconstruction before calculating the diffusion parameters was to register the different diffusion-weighted images. A sub-voxel image registration algorithm was selected that uses cross-correlation of the Fourier transform of the images that is freely available in Matlab [23, 24].

This registration method allows for sub-voxel accurate translation registration of the images.

Articular cartilage was segmented in the b_0 images (T2-weighted images) using in-house software PaCaSe [21]. After identifying the maximum height of the intercondylar fossa, the femoral cartilage was then subdivided into the trochlea, the lateral condyle, and the medial condyle. In total, we considered six cartilage plates for our analysis: femoral trochlea (FT), lateral femoral condyle (LFC), medial femoral condyle (MFC), medial tibia (MT), lateral tibia (LT), and the patella (P). Mean and standard deviation of MD and FA were calculated for each cartilage plate.

MD and FA were calculated using custom routines from the motion-corrected diffusion-weighted images [25]. The impact in MD and FA of each processing step was assessed through the average MD and FA values of the medial femoro-tibial compartment of healthy ($n = 5$, KL 0) and OA KL 2 subjects ($n = 6$) without correction, after motion correction, and after motion correction plus registration.

The signal-to-noise ratio (SNR) was calculated by dividing the signal intensity by the standard deviation of noise, σ. Since no filters were used and the channels were combined using the sum of squares, σ was calculated by fitting a noncentral χ^2 distribution to the background noise [26].

Statistical analysis

Paired and unpaired t test were used to compare two groups of parameters (e.g., derived from OA vs. healthy subjects) after the data was confirmed as normally distributed via the non-parametric Kolmogorov-Smirnov test. Comparisons of more than two groups (e.g., differences across cartilage plates) were performed with the one-way analysis of variance (ANOVA) test with Bonferroni correction. The concordance correlation coefficient (ρ_c) was used to measure the level of agreement of the diffusion measurements at different temperatures with those derived from the literature [27]. Bland-Altman plots were used to compare RAISED diffusion measurements with single-shot diffusion-weighted EPI as a standard of reference. Test-retest reproducibility was reported as the root mean square of the coefficient of variation over the three scans for each parameter and cartilage plate. An overall p value of 0.05 was chosen to indicate statistical significance.

Results

Validation of the RAISED pulse sequence

When compared with the diffusivity of free water published in the literature, the measurement of diffusivity in MR scanner

showed a high concordance correlation coefficient (ρ_c) of 0.996 with a 95% confidence interval (0.985, 0.999) (Fig. 2). The root mean square error of the measured diffusivity was 0.028×10^{-3} mm^2/s corresponding to 1.28% error (range -1.8 to 2.1%).

There was no measurable effect due to eddy currents. Differences in signal intensity of images acquired with opposite polarity of the diffusion gradients was $+ 0.06 \pm 0.20\%$, and differences of acquisitions with the same polarity was $- 0.01 \pm 0.15\%$. There was no statistical significance between images of the same and opposite polarity.

The average geometric difference of the segmentations of the images acquired with opposite polarities was 0.07 ± 0.11 mm, equivalent to 10% of in-plane resolution, which was not different to the differences between same-polarity repeated segmentations (0.06 ± 0.09 mm). Differences in MD and FA calculated from acquisitions with opposite diffusion gradient directions were ($1.9 \pm 0.8\%$) and ($3.3 \pm 1.2\%$), similar to the error produced by rescanning with the same gradient polarity (MD $1.7 \pm 0.3\%$, FA $3.1 \pm 0.7\%$). SNR of phantom measurements was 38.0 ± 7.2, slightly higher than in our in vivo measurements (see "Motion correction").

Comparison of EPI and motion-corrected RAISED diffusion parameters showed no statistically significant bias neither in MD ($p = 0.17$, difference in MD = [0.011 ± 0.041] × 10^{-3} mm^2/s, average coefficient of variation [CV] = 1.8%), nor in FA ($p = 0.08$, difference FA = 0.015 ± 0.045, average CV = 7.5%). Figure 2 shows Bland-Altman plots of MD and FA values acquired with EPI as our standard of reference and RAISED pulse sequences with (left column) and without (right column) motion correction.
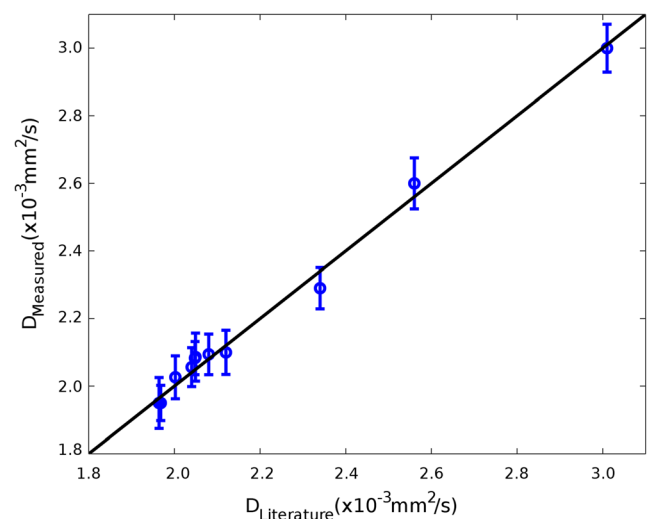

Fig. 2 Mean diffusivity of water phantoms at different temperatures and comparison with literature values. The graph represents the MD from the literature in the abscissa and the MD measured with the RAISED sequence on the ordinate. Bars represent twice the standard deviation

Participants

Healthy volunteers included three female and three male subjects with a mean age of 43.5 ± 6.5 years (range 32–57 years), BMI 26.9 ± 5.1 kg/m^2 (range 23.3–34.8 kg/m^2). Eighteen OA patients were included with mean age 55.0 ± 7.6 years (range 45–67 years), and average BMI of 26.8 ± 7.3 kg/m^2 (range 21.0–42.7 kg/m^2). Nine OA subject were classified as KL grade 1 (five female, age 53.8 ± 5.9 years, BMI: 26.7 ± 3.8 kg/m^2) and nine as KL grade 2 (six female, age: 56.2 ± 9.6 years, BMI: 26.9 ± 5.2 kg/m^2). One-way ANOVA did show a statistical significant difference in age among the groups ($p < 0.016$), but no BMI difference. Healthy volunteers were significantly younger than OA patients ($p = 0.002$), but there was no age difference between the KL 1 and KL 2 groups ($p = 0.61$). The difference in BMI between the healthy and OA groups did not reach statistical significance.

Motion correction

Figures 3 and 4 illustrate the importance of motion correction. The lack of motion correction led to clear
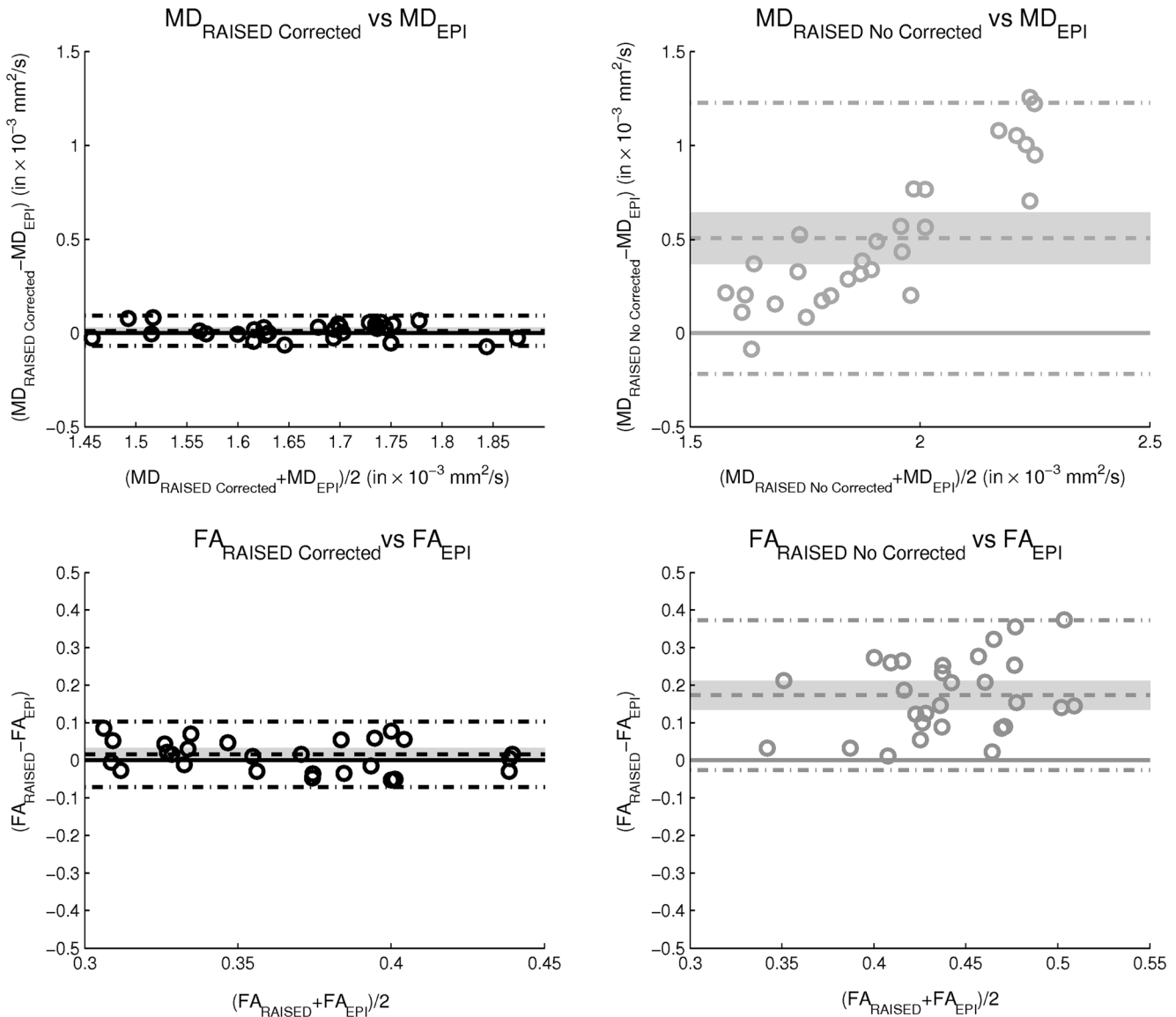

Fig. 3 Bland-Altman plots comparing the diffusion parameters measured with the RAISED sequence with (dark gray) and without (light gray) correction against the values obtained with a single-shot diffusion-weighted EPI. The thick solid line corresponds to zero difference between RAISED and EPI measurements, the dashed line represents the mean difference between RAISED and EPI, and the dot-dash line the two-sigma range of the difference. The 95% confidence interval of the mean is indicated by the light gray area around the mean difference. RAISED values will be biased against the EPI standard of reference if the zero difference line lies outside the 95% confidence interval of the mean (light gray area). MD and FA measured with RAISED after using motion correction do not have a significant bias compared to the EPI parameters ($p > 0.05$), but there is a significant bias in the measurements if motion correction is not applied
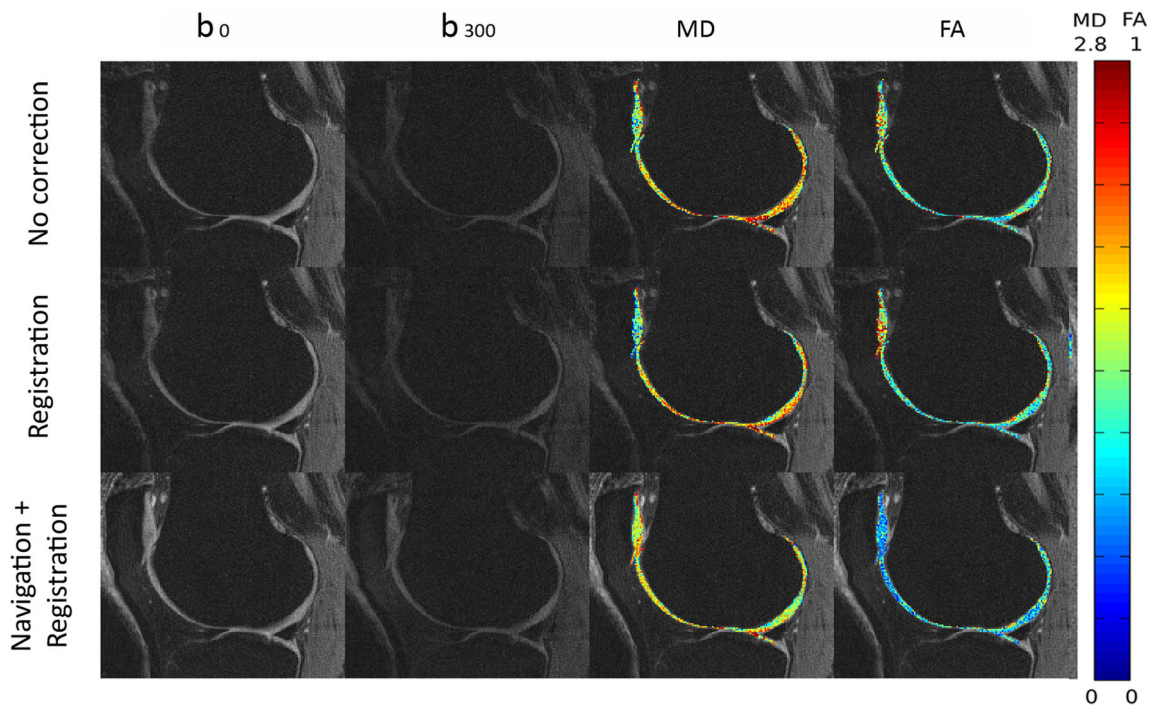
Fig. 4 Example of image correction in MD and FA cartilage values. From left to right, the images include the $b = 0$ and $b = 300$ s/mm² images, as well as MD and FA maps overlaid on the $b = 0$ s/mm² image. The top row shows reconstructed images without correction. The middle row contains images after registration, which only aligns the b_{300} images to the b_0 changing the MD and FA values in the thin cartilage layer. The bottom row shows images after motion correction and registration. Notice the higher intensity in the cartilage in the $b = 300$ s/mm² diffusion-weighted image and how the area of the patella is better defined in both images. This results in lower MD and FA. MD is in units of $\times 10^{-3}$ mm²/s

signal loss that was most pronounced in the muscles and the anterior region of the knee in 83% of the images. Not registering motion-corrected images introduces characteristic bands of abnormal MD and FA. The average displacement correction increased with the slice number from 0%, 10%, 28%, 47%, 58%, 66%, and 76% of the voxel size.

Table 1 shows the effect of motion correction and registration in the TM and MFC of KL 0 ($n = 5$) and KL 2 ($n = 6$) subjects. Without motion correction, MD of the femur and tibia of OA subjects was only + 11% and + 13% higher than that of healthy subjects and did not achieve statistical significance. Motion correction resulted in reduced mean MD and FA with less group variance in both groups (control MD/FA decreased -16.6/-14.1%; OA MD/FA decreased -7.6/-18.4%), achieving statistical significance (two sided t test, $p < 0.05$).

The mean SNR of the b_0 and the diffusion-weighted images across all subject was 18.3 ± 1.2, 16.5 ± 1.5, and 18.4 ± 2.7 for the femur tibia and patella respectively. Diffusion-weighted images presented SNR values larger than 10 in all cartilage plates (11.5 ± 0.8 for the femur, 10.4 ± 0.9 for the tibia, and 11.4 ± 1.5 for the patella). There were no significant differences in SNR between healthy and OA subjects in any cartilage region.

Diffusion in healthy and OA subjects

Figure 5 shows parameter maps from healthy and KL 1 and 2 OA subjects. The average MD and FA values per cartilage plate for KL 0, 1, and 2 subjects are summarized in Table 2 and a boxplot of the femoro-tibial compartment is shown in Fig. 6. Both Table 2 and Fig. 6 show a trend of increased MD and decreased FA with the KL grade. The medial compartment (MFC and TM) had the largest variations in OA subjects. We found significant increased MD in the LFC (+ 7%) and in the MFC (+ 9%) for KL 1 subjects and in the medial (TM + 17%; MFC + 11%) and lateral compartments (TL + 12% LFC + 10%) for KL 2 subjects. FA was significantly lower in the MFC (-11%) of KL 1 subjects, and on the patello-femoral (FT -14%; P -18%), lateral (TL -1%; LFC -14%) and medial (MFC -13%) compartments in KL 2 subjects. Test-retest reproducibility is summarized in Table 3 and was below 4% for MD and 6% for FA for all cartilage plates but for the patella. There were no differences between the same-day or short-term reproducibility or between KL 0 and KL > 0 subjects.

Discussion

We have implemented and validated the RAISED sequence with a non-linear motion correction algorithm for DTI of

Table 1 Change of average MD and FA values with the processing steps

		MD			FA		
		No correct.	Nav.	Nav.+reg.	No correct.	Nav.	Nav.+reg.
Healthy	TM	1.53 (0.11)	1.39 (0.11)	1.38 (0.09)	0.46 (0.04)	0.45 (0.03)	0.46 (0.05)
OA	TM	1.77 (0.23)	1.71 (0.19)	*1.62 (0.19)*	0.41 (0.05)	0.36 (0.07)	0.42 (0.05)
Healthy	MFC	1.67 (0.13)	1.50 (0.09)	1.46 (0.04)	0.53 (0.07)	0.52 (0.03)	0.42 (0.02)
OA	MFC	1.74 (0.12)	1.70 (0.11)	*1.60 (0.09)*	0.46 (0.03)	*0.40 (0.04)*	*0.37 (0.02)*

Italicized numbers represent statistically significant difference between the healthy and OA subjects (*t* test, $p < 0.05$). *No Correct.*, reconstruction without correction; *Nav.*, reconstruction with motion correction; *Nav.+reg.*, reconstruction including motion correction and sub-voxel registration. MD in units of $\times 10^{-3}$ mm^2/s

articular cartilage. Our validation shows that RAISED sequence with a non-linear phase correction provides a repeatable measurement of diffusion parameters, with negligible influence from eddy current or motion artifacts, and with potential for the early diagnosis of OA.

Motion artifacts in radial sequences lead to decreased signal intensity due to incoherent addition of radial views (spokes) that contain inconsistent phase information. Since motion artifacts in radial images are smeared in all directions, artifacts are much less striking than typical motion ghosting in Cartesian sequences. Our results show that motion correction

is critical in recovering the signal loss and in providing accurate diffusion values, even for moderate *b* values. Miller et al first illustrated the need for motion correction in diffusion-weighted imaging of articular cartilage using a 3D steady state diffusion-weighted imaging (SSDWI) sequence with effective *b* values up to 630 s/mm^2 [28]. However, most of the studies,

Table 2 Averaged MD and FA per cartilage region and KL score

Cartilage	Parameter	KL 0 ($n = 6$)	KL 1 ($n = 9$)	KL 2 ($n = 9$)
TL	MD	1.40 (0.07)	1.51 (0.13)	*1.57 (0.15)*
		[1.33–1.48]	[1.30–1.71]	[1.35–1.87]
	FA	0.46 (0.05)	0.42 (0.04)	*0.41 (0.04)*
		[0.42–0.53]	[0.37–0.47]	[0.34–0.45]
TM	MD	1.34 (0.14)	1.48 (0.18)	*1.57 (0.19)*
		[1.13–1.48]	[1.24–1.83]	[1.38–1.91]
	FA	0.49 (0.10)	0.44 (0.03)	0.42 (0.05)
		[0.38–0.60]	[0.41–0.48]	[0.34–0.50]
LFC	MD$^\perp$	1.47 (0.10)	*1.58 (0.09)*	*1.62 (0.08)*
		[1.40–1.58]	[1.44–1.69]	[1.48–1.77]
	FA$^\perp$	0.43 (0.05)	0.38 (0.04)	*0.37 (0.02)*
		[0.37–0.53]	[0.32–0.45]	[0.33–0.40]
MFC	MD$^\perp$	1.44 (0.07)	*1.56 (0.08)*	*1.60 (0.09)*
		[1.30–1.53]	[1.44–1.69]	[1.45–1.75]
	FA$^\perp$	0.44 (0.04)	*0.39 (0.02)*	*0.39 (0.02)*
		[0.40–0.46]	[0.36–0.42]	[0.34–0.41]
FT	MD	1.48 (0.07)	1.59 (0.16)	1.57 (0.13)
		[1.40–1.59]	[1.34–1.81]	[1.42–1.82]
	FA$^\perp$	0.45 (0.05)	0.41 (0.04)	*0.39 (0.03)*
		[0.39–0.50]	[0.37–0.45]	[0.34–0.43]
P	MD	1.50 (0.11)	1.62 (0.12)	1.63 (0.20)
		[1.40–1.67]	[1.48–1.83]	[1.36–2.03]
	FA$^\perp$	0.44 (0.04)	0.40 (0.03)	*0.37 (0.06)*
		[0.38–0.47]	[0.37–0.47]	[0.29–0.48]

Averaged values given as the mean, the standard deviation in brackets, and the range from minimum to maximum in square brackets. MD in units of $\times 10^{-3}$ mm^2/s. Italicized numbers indicate significant difference to the control group (*t* test, $p < 0.05$)

$^\perp$ One-way ANOVA significance ($p < 0.05$) for all three group comparison
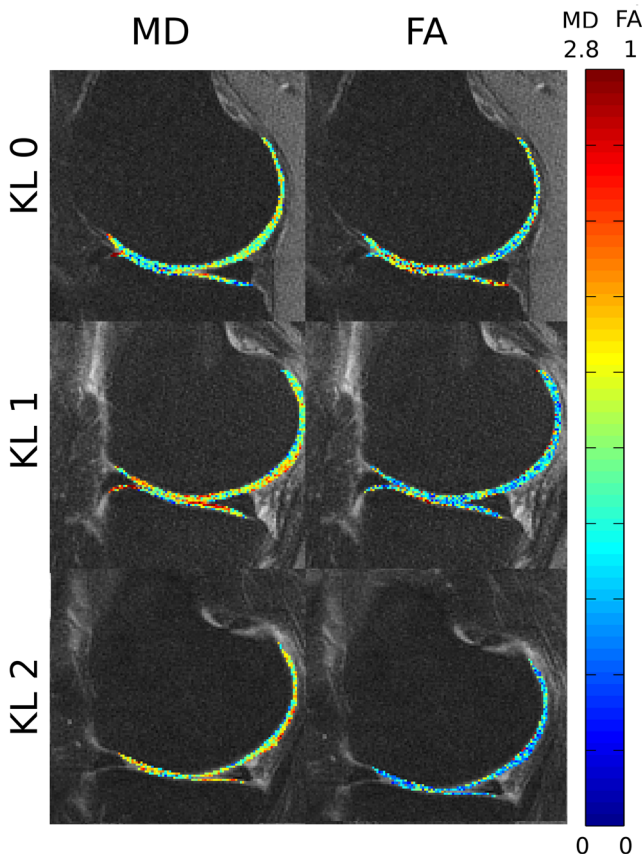
Fig. 5 Example of MD and FA maps on healthy and OA subjects with KL 0, 1, and 2 showing increasing MD and decreasing FA with KL grade
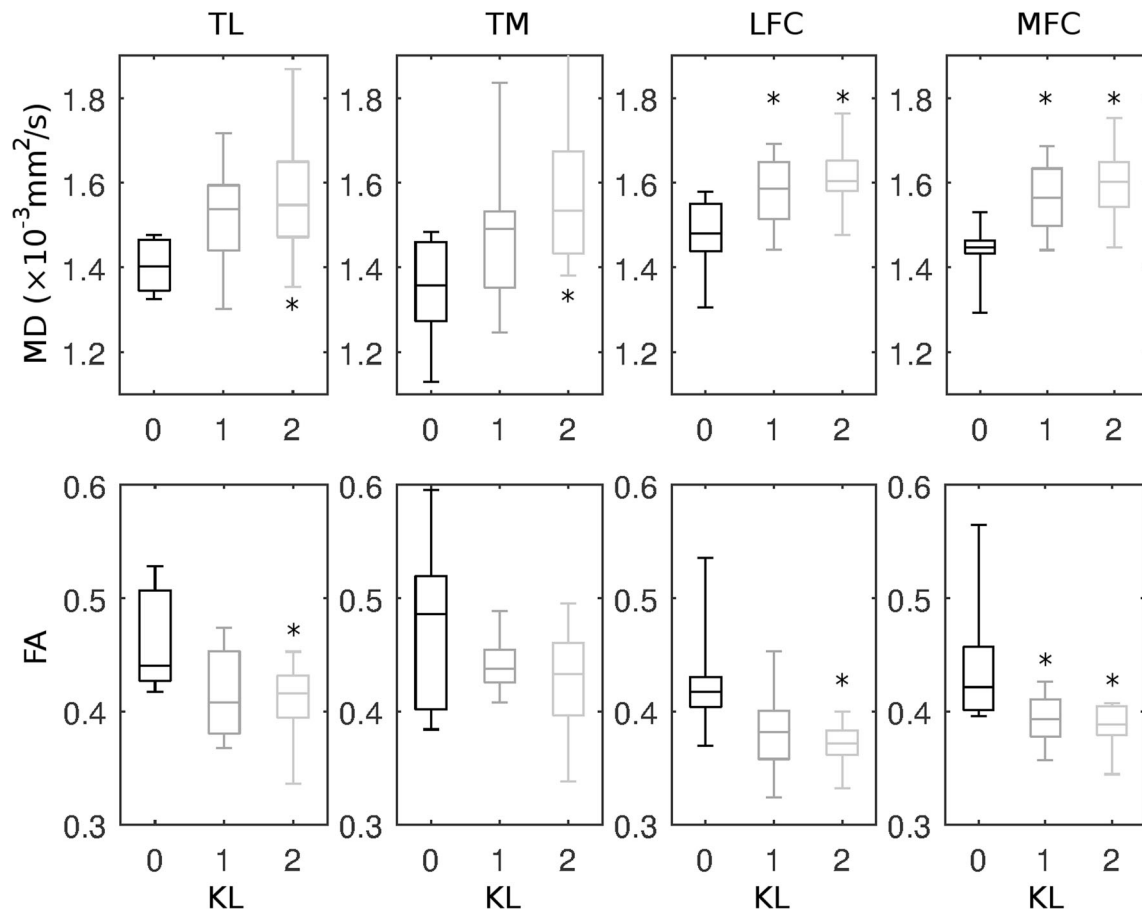
Fig. 6 Boxplot of average MD and FA of the tibiofemoral compartment for different KL grades. Data shows increased MD and decreased FA in MFC and LFC both in KL 1, KL 2 subjects and in TM and TL in the KL 2 group

which used multi-shot sequences for diffusion quantification, did not use any navigation correction [8, 29–31].

A non-linear phase correction represents an optimal approach to correct motion in the knee joint. Here, we implemented the method developed by Miller and Pauly, for which a 2D navigator needs to be acquired after each spoke [12]. Optimization of the 2D-EPI navigator was needed to provide adequate image quality. Since navigators are of low resolution (32×32 in our case), we acquired all lines in the same readout direction to avoid N/2 ghosting artifacts. To reduce echo time, we used partial Fourier 6/8 and a relative high bandwidth (800 Hz/pixel) that also helped reduce off-resonant artifacts in the phase encoding. To further reduce image distortions around

Table 3 Test-retest reproducibility (%)

	Global	FT	LFC	MFC	TL	TM	P
MD	3.54	3.98	3.52	3.45	2.93	3.12	7.16
FA	5.34	6.10	5.69	5.53	4.72	4.63	10.81

Root mean square of the coefficient of variation over the 6 subjects (3 Healthy, 3 OA)

cartilage, we found that the best phase-encoding direction was head-foot for images acquired in the sagittal and coronal planes, and anterior-posterior for axial images.

One last important processing step is image registration. Small misalignments of the diffusion-weighted images around the millimeter range articular-cartilage thickness can cause artificially high or low diffusion values. RAISED acquires diffusion-weighted images subsequently, and we observed a linear increasing misalignment of the images. We measured the misalignment for different diffusion directions and slice orientations and found very similar displacements. However, we observed a consistent shift in the frequency of the water peak of ~120 Hz before and after RAISED measurement. Thus, the observed misalignment is likely due to a drift in the scanner hardware caused by the intensive use of the gradients.

The MD and FA values measured in articular cartilage of healthy volunteers have similar ranges to previous studies published which use methods that are not motion sensitive, such as the EPI, a 3D SSDWI, or line scan diffusion tensor sequence [32]. We also found differences between healthy and OA subjects, consistent with previous studies (+ 15% increase in MD and -12% reduction in

FA) at 7 T or 3 T [9, 10, 33]. Once more, these differences could be only detected after motion correction and registration. Our diffusion metrics have a reproducibility error below 5%, which is in line with the reproducibility of many other parameters used for cartilage such as T2 (1.0–4.0%), T1rho (3.9–5.0%), sodium imaging (7.5–13.6%), and delayed gadolinium enhanced MRI of cartilage (dGEMRIC, 4.2–5.5%) [34–39]. FA showed worse reproducibility than MD, which is to be expected, since FA is a measure of eigenvalue dispersion and thus more sensitive to noise. The worst test-retest values were found in the patella due to the partial-volume effects that arise because of the curved cartilage surface.

One last issue to discuss is the b value of the diffusion-weighted images. In this work, diffusion-weighted images were acquired with a b value of 300 s/mm^2, which is lower than the optimal b value given by $b\sim 1/D$. Assuming an average diffusivity of 1.5×10^{-3} mm^2/s, the optimal b value would be around 666 mm^2/s. Previous studies have used b values in the range of 160–650 s/mm^2 in vivo with slice thickness between 3 and 4 mm [8, 28, 29, 31, 33, 40]. The selection of a sub-optimal b value was dictated by necessity for adequate SNR (> 10) in the diffusion-weighted images. A SNR of ten in the diffusion-weighted images with six diffusion directions can provide accurate cartilage-plate estimates, [25] although it can be insufficient for more accurate pixel-wise comparisons, especially for the FA, which is more sensitive to noise. The use of a much higher through-plane than in-plane resolution is a common practice in the field of quantitative imaging biomarkers of articular cartilage and can result in partial-volume effects.

This work has some limitations. First, our in vitro validation only tested indirectly the absence of eddy current artifacts, but no direct measurement of fields could be made. Second, we only included a limited number of subjects to show feasibility of the technique. However, despite the small number of subjects, we could see some group differences indicating the potential of the method. Third, the healthy population was BMI-matched to the OA groups but significantly younger (~ 10 years) than the OA population, which could contribute to increased group differences.

In summary, RAISED sequence with the proposed reconstruction framework provides reproducible assessment of DTI parameters in vivo at 3 T with potential to detect early stages of the disease.

Compliance with ethical standards

The content is solely the responsibility of the authors and does not necessarily represent the official views of the NIH.

Guarantor The scientific guarantor of this publication is José G Raya, PhD.

Conflict of interest The authors of this manuscript declare no relationships with any companies, whose products or services may be related to the subject matter of the article.

Statistics and biometry One of the authors has significant statistical expertise.
No complex statistical methods were necessary for this paper.

Informed consent Written informed consent was obtained from all subjects (patients) in this study.

Ethical approval Institutional Review Board approval was obtained.

Methodology
• prospective
• case-control study
• performed at one institution

References

1. Filidoro L, Dietrich O, Weber J et al (2005) High-resolution diffusion tensor imaging of human patellar cartilage: feasibility and preliminary findings. Magn Reson Med 53:993–998
2. Meder R, de Visser SK, Bowden JC, Bostrom T, Pope JM (2006) Diffusion tensor imaging of articular cartilage as a measure of tissue microstructure. Osteoarthritis Cartilage 14:875–881
3. de Visser SK, Bowden JC, Wentrup-Byrne E et al (2008) Anisotropy of collagen fibre alignment in bovine cartilage: comparison of polarised light microscopy and spatially resolved diffusion-tensor measurements. Osteoarthritis Cartilage 16:689–697
4. Raya JG, Melkus G, Adam-Neumair S et al (2011) Change of diffusion tensor imaging parameters in articular cartilage with progressive proteoglycan extraction. Invest Radiol 46:401–409
5. Raya JG, Melkus G, Adam-Neumair S et al (2013) Diffusion-tensor imaging of human articular cartilage specimens with early signs of cartilage damage. Radiology 266:831–841
6. Deng X, Farley M, Nieminen MT, Gray M, Burstein D (2007) Diffusion tensor imaging of native and degenerated human articular cartilage. Magn Reson Imaging 25:168–171
7. Ferizi U, Rossi I, Lee Y et al (2017) Diffusion tensor imaging of articular cartilage at 3T correlates with histology and biomechanics in a mechanical injury model. Magn Reson Med 78:69–78
8. Guha A, Wyatt C, Karampinos DC, Nardo L, Link TM, Majumdar S (2015) Spatial variations in magnetic resonance-based diffusion of articular cartilage in knee osteoarthritis. Magn Reson Imaging 33:1051–1058
9. Raya JG, Dettmann E, Notohamiprodjo M, Krasnokutsky S, Abramson S, Glaser C (2014) Feasibility of in vivo diffusion tensor imaging of articular cartilage with coverage of all cartilage regions. Eur Radiol 24(7):1700–1706
10. Raya JG, Horng A, Dietrich O et al (2012) Articular cartilage: in vivo diffusion-tensor imaging. Radiology 262:550–559
11. Berstein MA, King KF, Zhou XJ (2004) Chapter 14 − Basic pulse sequences. In: Berstein MA, King KF, Zhou XJ (eds) Handbook of MRI pulse sequences, 1st edition
12. Miller KL, Pauly JM (2003) Nonlinear phase correction for navigated diffusion imaging. Magn Reson Med 50:343–353

13. Skare S, Hedehus M, Moseley ME, Li TQ (2000) Condition number as a measure of noise performance of diffusion tensor data acquisition schemes with MRI. J Magn Reson 147:340–352

14. Mills R (1973) Self-diffusion in normal and heavy water. J Phys Chem 77:685–688

15. Tofts PS, Lloyd D, Clark CA et al (2000) Test liquids for quantitative MRI measurements of self-diffusion coefficients in vivo. Magn Reson Med 43:368–374

16. Gillen KT, Douglass DC, Hoch MJR (1972) Self-diffusion in liquid water to -31°C. J Chem Phys 57:5117–5119

17. Harris KR, Woolf LA (1980) Pressure and temperature dependence of the self diffusion coefficient of water and oxygen-18 water. J Chem Soc Faraday Trans 76:377–385

18. Dietrich O (2018) Diffusion coefficients of water. Available via http://dtrxde/od/diff/. Accessed 2018-07-08 2018

19. Bodammer N, Kaufmann J, Kanowski M, Tempelmann C (2004) Eddy current correction in diffusion-weighted imaging using pairs of images acquired with opposite diffusion gradient polarity. Magn Reson Med 51:188–193

20. Neeman M, Freyer JP, Sillerud LO (1991) A simple method for obtaining cross-term-free images for diffusion anisotropy studies in NMR microimaging. Magn Reson Med 21:138–143

21. König L, Groher M, Keil A, Glaser C, Reiser M, Navab N (2007) Semi-automatic segmentation of the patellar cartilage in MRI. Bildverarbeitung für die Medizin 17:404–408

22. Altman R, Asch E, Bloch D et al (1986) Development of criteria for the classification and reporting of osteoarthritis. Classification of osteoarthritis of the knee. Diagnostic and Therapeutic Criteria Committee of the American Rheumatism Association. Arthritis Rheum 29:1039–1049

23. Guizar-Sicairos M (2008) Efficient subpixel image registration by cross-correlation https://www.mathworks.com/matlabcentral/fileexchange/18401-efficient-subpixel-imageregistration-by-cross-correlation?requestedDomain=www.mathworks.com. Accessed 1 Jan 2016

24. Guizar-Sicairos M, Thurman ST, Fienup JR (2008) Efficient subpixel image registration algorithms. Opt Lett 33:156–158

25. Ferizi U, Ruiz A, Rossi I, Bencardino J, Raya JG (2018) A robust diffusion tensor model for clinical applications of MRI to cartilage. Magn Reson Med 79:1157–1164

26. Constantinides CD, Atalar E, McVeigh ER (1997) Signal-to-noise measurements in magnitude images from NMR phased arrays. Magn Reson Med 38:852–857

27. Lin LI (1989) A concordance correlation coefficient to evaluate reproducibility. Biometrics 45:255–268

28. Miller KL, Hargreaves BA, Gold GE, Pauly JM (2004) Steady-state diffusion-weighted imaging of in vivo knee cartilage. Magn Reson Med 5:394–398

29. Bieri O, Ganter C, Scheffler K (2012) Quantitative in vivo diffusion imaging of cartilage using double echo steady-state free precession. Magn Reson Med 68:720–729

30. Heule R, Ganter C, Bieri O (2014) Rapid estimation of cartilage T with reduced T sensitivity using double echo steady state imaging. Magn Reson Med 71(3):1137–1143. https://doi.org/10.1002/mrm.24748

31. Staroswiecki E, Granlund KL, Alley MT, Gold GE, Hargreaves BA (2012) Simultaneous estimation of T(2) and apparent diffusion coefficient in human articular cartilage in vivo with a modified three-dimensional double echo steady state (DESS) sequence at 3 T. Magn Reson Med 67:1086–1096

32. Raya JG (2015) Techniques and applications of in vivo diffusion imaging of articular cartilage. J Magn Reson Imaging 41:1487–1504

33. Azuma T, Nakai R, Takizawa O, Tsutsumi S (2009) In vivo structural analysis of articular cartilage using diffusion tensor magnetic resonance imaging. Magn Reson Imaging 27:1242–1248

34. Glaser C, Mendlik T, Dinges J et al (2006) Global and regional reproducibility of T2 relaxation time measurements in human patellar cartilage. Magn Reson Med 56:527–534

35. Raya JG, Horng A, Dietrich O et al (2009) Voxel-based reproducibility of T2 relaxation time in patellar cartilage at 1.5 T with a new validated 3D rigid registration algorithm. MAGMA 22:229–239

36. Madelin G, Babb JS, Xia D, Chang G, Jerschow A, Regatte RR (2012) Reproducibility and repeatability of quantitative sodium magnetic resonance imaging in vivo in articular cartilage at 3 T and 7 T. Magn Reson Med 68:841–849

37. Multanen J, Rauvala E, Lammentausta E et al (2009) Reproducibility of imaging human knee cartilage by delayed gadolinium-enhanced MRI of cartilage (dGEMRIC) at 1.5 Tesla. Osteoarthritis Cartilage 17:559–564

38. Jordan CD, McWalter EJ, Monu UD et al (2014) Variability of CubeQuant T1rho, quantitative DESS T2, and cones sodium MRI in knee cartilage. Osteoarthritis Cartilage 22:1559–1567

39. Gupta R, Virayavanich W, Kuo D et al (2014) MR T(1)rho quantification of cartilage focal lesions in acutely injured knees: correlation with arthroscopic evaluation. Magn Reson Imaging 32:1290–1296

40. Xu J, Xie G, Di Y, Bai M, Zhao X (2011) Value of T2-mapping and DWI in the diagnosis of early knee cartilage injury. J Radiol Case Rep 5:13–18